Macromolecules
ARTICLE

Macromolecules **2010**, *43*, 4909–4920 **4909**
DOI: 10.1021/ma100333e

Iron Tris(dibenzoylmethane−polylactide)

Jianbin Chen, Jessica L. Gorczynski, Guoqing Zhang, and Cassandra L. Fraser*

Department of Chemistry, University of Virginia, McCormick Road, Charlottesville, Virginia 22904

Received February 9, 2010; Revised Manuscript Received April 6, 2010

ABSTRACT: The polymeric metal complex iron tris(dibenzoylmethane-polylactide), $Fe(dbmPLA)_3$, was synthesized from D,L-lactide and $Fe(dbmOH)_3$, a hydroxyl functionalized metalloinitiator. Reactions are fast relative to those with the dbmOH ligand initiator even when no $Sn(oct)_2$ or DMAP catalyst is added, indicating that iron serves as both a dbm protecting group and a catalyst for lactide ring-opening polymerization (ROP). Kinetics experiments show good molecular weight control to ~60−70% conversion (e.g., PDIs < 1.1; no evidence of transesterification via ^{1}H NMR spectroscopic analysis; continued chain growth when $Fe(dbmPLA)_3$ is heated with additional lactide monomer). For comparison, $Fe(bdk)_3$ (bdk = β-diketonate) complexes were tested as lactide ROP catalysts using dbmOH and benzyl alcohol as the initiators. The red-orange $Fe(dbmPLA)_3$ polymers were analyzed by GPC, ^{1}H NMR and UV-vis spectroscopy. Demetalation with dilute HCl yields dbmPLA macroligands for chelation to other metals. The polymerization mechanism using $Fe(dbmOH)_3$ as an initiator and catalyst is also discussed and results suggest ligand exchange prior to initiation may be involved.

Introduction

Many living organisms utilize metalloproteins in essential life functions such as structure formation, catalysis, and electron and oxygen transport. For example, iron catalyzed reactions often require both Fe(II) and Fe(III) states, and in some cases iron species can form toxic hydroxide radicals and other reactive oxygen species. To avoid this problem and safely harness the unique redox, reactive, and physical properties of iron, in nature iron is typically encapsulated into macromolecules where its chemistry and properties can be precisely controlled. Inspired by such metalloproteins, polymeric metal complexes (PMCs) featuring well-defined polymeric ligands bound to metal centers have been designed and synthesized. This type of organic/inorganic hybrid material combines the versatile functionalities of metal complexes (e.g., color, magnetism, luminescence, reactivity) with those of polymers (e.g., assembly behavior, processability), and can also exhibit diverse structures and properties.[1,2]

To prepare PMCs, convergent methods, such as macroligand chelation or metal complex-polymer coupling, or divergent approaches, such as metal complex initiation can be used.[3] Challenges with the former methods include the presence of multiple macromolecular components, namely reactants and products that are hard to separate if reactions do not go cleanly to completion. Therefore, the initiation approach is preferred for obtaining more homogeneous materials. Sometimes metal catalysts can result in sample contamination,[4] and thus a self-catalyzing initiator for PMC synthesis is desirable. Using ring-opening polymerization (ROP) reactions to prepare well-defined PMC materials can be beneficial due to the living/controlled nature of certain systems. For example, metal alkoxide-initiated ε-caprolactone ROP begins with coordination of the carbonyl oxygen of the monomer to the empty orbitals of the metal Lewis acid, followed by cleavage of the acyl oxygen bond, or insertion of ε-caprolactone into the metal−alkoxo oxygen bond. Therefore, metal initiators may also work as catalysts. Tributyltin methoxide (Bu_3SnOMe)[5] can initiate and catalyze the ROP of lactide and ε-caprolactone, as can other metal alkoxides including magnesium ethoxide, aluminum 2-propoxide, zinc *n*-butoxide, titanium *n*-butoxide, and zirconium *n*-propoxide.[6] However, ROP of esters with these reported metal alkoxide catalysts results in broad molecular weight distributions because propagation is faster than initiation and intramolecular transesterification reactions can occur. Therefore, the development of a more efficient and controlled self-catalyzing ROP system for PMC preparation could be useful and previous reports with iron catalysts for ROP[7] suggest that "built-in" iron β-diketonates could be a viable catalytic route.

Given the renewable and biodegradable nature of poly(lactic acid) (PLA) and the prevalence of iron in biology, using PLA as building blocks and iron for coordination in PMC synthesis can lead to a new kind of biomaterial. Many iron compounds are regarded as less harmful than other heavy metal complexes,[7,8] and thus, can be suitable for biomedical applications. The red $Fe(dbm)_3$ complexes are sensitive to acid, and thus can be useful as functional elements in responsive materials. Iron dbm complexes are also potential bioactive agents, reported as cancer therapeutics.[9] In a previous communication,[10] an alcohol-functionalized iron(III) tris(dibenzoylmethane) complex, $Fe(dbmOH)_3$, possessed initiator, dbm protecting group, and lactide ROP catalyst functions. In this case, no additional metal alkoxide catalysts (e.g., tin,[11] aluminum,[12] bismuth,[13] or lanthanides[14]) or solvent were used and well-defined orange $Fe(dbmPLA)_3$ metallopolymers were achieved in good yield. As chromophores and acid sensitive structural features in the resulting material, the iron complexes combine multiple functions in a single reagent and material.

Iron centered polymers may also serve as precursors to metal free dbm end-functionalized polymers or macroligands. In this case, iron acts a protecting group for β-diketonate sites. Starting from $Fe(dbmPLA)_3$, the dbmPLA macroligand is conveniently generated through acidification.[10] By comparison, direct initiation with dbmOH using $Sn(oct)_2$ for lactide or ε-caprolactone[15,16] ROP exhibits slow reaction rate and less control possibly due to the diketone binding to tin and altering the catalytic activity.

*To whom correspondence should be addressed. E-mail: fraser@virginia.edu.

Published on Web 05/07/2010

Although we have also explored the difluoroboron moeity as a protecting group for dbm in macroligand synthesis, and ROP with BF_2dbmOH is significantly faster than with unprotected dbmOH,[17] Fe^{3+}, has the advantage of protecting not just one, but three equivalents of dbmOH with fast and easy postpolymerization modification, namely metal removal. In addition to their synthetic value as polymeric building blocks for modular synthesis, diketonate macroligands are also desirable targets for their properties as well. Recently it was found that metal-free dbmPLA is dual emissive, exhibiting both fluorescence and rare room-temperature phosphorescence in the solid state,[17] sparking increased interest in the photophysics of β-diketones in solid-state polymers. These results with dbmPLA and the "iron as a protecting group" synthetic route may extend to other diketone and polymer systems as well.

Following up on our initial communication,[10] here a more detailed study of the synthesis and characterization of the Fe(dbmOH)$_3$ metalloinitiator, Fe(dbmPLA)$_3$, and the corresponding deprotected dbmPLA macroligand product were performed. Kinetics studies on the polymerization and structural characterization of the PMCs were carried out as well. Finally, control experiments were run to gain some insight into the polymerization mechanism.

Experimental Section

Materials. 3,6-Dimethyl-1,4-dioxane-2,5-dione (D,L-lactide, Aldrich) and (3*S*)-*cis*-3,6-dimethyl-1,4-dioxane-2,5-dione (L-lactide, Aldrich) were recrystallized twice from ethyl acetate and stored under nitrogen. Dry tetrahydrofuran (THF) and methylene chloride (CH_2Cl_2) were obtained by passage through alumina columns. Anhydrous $FeCl_3$ (Aldrich, 99+%) and NaH (Aldrich, 95%) were stored under nitrogen. Tin(II) 2-ethylhexanoate (Sn(oct)$_2$, Spectrum), benzyl alcohol (BnOH, 99+%, Aldrich), and all other reagents were used as received without further purification. 1-[4-(2-Hydroxyethoxy)-phenyl]-3-phenyl-propane-1,3-dione (dbmOH) (**1**) was synthesized as previously reported.[20]

Methods. ^{1}H NMR (300 MHz) and ^{13}C NMR (75 MHz) spectra were recorded on either a Varian UnityInova 300/54 or Varian MercuryPlus 300/54 instrument in $CDCl_3$. Homonuclear-decoupled ^{1}H NMR (500 MHz) spectra were recorded on a Varian UnityInova 500/51 instrument in $CDCl_3$. ^{1}H NMR spectra were referenced to the signal for residual protio chloroform at 7.260 ppm. Molecular weights were determined by one of two GPC instruments. The first, for the dbmPLA samples (THF, 25 °C, 1.0 mL/min) employed multiangle laser light scattering (MALLS) (λ_{max} = 633 nm, 25 °C), refractive index (RI) (λ_{max} = 633 nm, 40 °C), and UV-vis diode-array detection using Polymer Laboratories 5 μm-mixed-C columns along with Wyatt Technology Corporation (Optilab DSP interferometric refractometer, Dawn DSP laser photometer) and Hewlett-Packard instrumentation (Series 1100 HPLC) and software (ASTRA). The incremental refractive index (dn/dc values) of dbmPLA was estimated to be 0.050 mL/g for molecular weight calculations using light scattering. Alternatively, molecular weight data was determined by a second GPC instrument (THF, 20 °C, 1.0 mL/min) using polystyrene standards with Polymer Laboratories 5 μm-mixed-C columns along with Hewlett-Packard instrumentation (Series 1100 HPLC) and Viscotek software (TriSEC GPC Version 3.0, Viscotek Corp.). Molecular weights were corrected for PS standard approximation of PLA (molecular weights multiplied by 0.58) as described.[18] Elemental analysis for C, H, and O was performed by Atlantic Microlab Inc., Norcross, GA. UV−vis spectra were recorded on a Hewlett-Packard 8452A diode-array spectrophotometer.

DbmPLA (2) (Sn(oct)$_2$ Catalyst). A representative procedure is provided. A dry, 25 mL Kontes flask was charged with dbmOH initiator **1** (0.251 g, 0.885 mmol) and D,L-lactide (6.35 g, 44.1 mmol). The flask was evacuated, backfilled with nitrogen, sealed, and placed in an oil bath set at 130 °C to produce a homogeneous melt. A 0.320 M solution of Sn(oct)$_2$ in hexanes (55 μL, 0.018 μmol) was added to the melt under a nitrogen atmosphere, and the flask was resealed and heated at 130 °C for 6.5 h. The resulting clear, viscous mixture was cooled to room temperature and dissolved in CH_2Cl_2 (~15 mL). The product was precipitated by dropwise addition of the CH_2Cl_2 solution to stirred, cold methanol (~150 mL). The supernatant liquor was decanted, and the solid residue that formed was precipitated twice from CH_2Cl_2/MeOH and once from CH_2Cl_2/hexanes, washed with cold methanol, and dried *in vacuo* to provide the PLA macroligand, dbmPLA (**2**) as a colorless foam: 5.06 g (77%). ^{1}H NMR (in $CDCl_3$) δ 16.96 (s, OH), 7.98 (d, 4 H, J = 8.8, 2′,6′-ArH, 2″,6″-ArH), 7.51 (m, 3 H, H-3″, H-4″, H-5″-ArH), 6.97 (d, 2 H, J = 8.8, 3′,5′-ArH), 6.80 (s, 1 H, CH), 5.10−5.31(m, CH), 4.52 (m, 2 H, ArOCH_2CH_2), 4.25 (t, 2 H, J = 4.4, ArOCH_2CH_2), 2.69 (broad s, 1 H, OH), 1.50−1.63 (d, J = 6.9, 336 H, CH_3), M_n(NMR) = 8 400, PDI = 1.12, M_w(MALLS) = 7 000.

DbmPLA (2) (DMAP Catalyst). The polymerization was performed according to the procedure for dbmPLA with Sn(oct)$_2$ except that DMAP (9.2 mg, 73.2 μmol) was used as the catalyst. The reaction mixture was heated for 0.5 h. The product was dried *in vacuo* to provide dbmPLA (**2**) as a pale yellow foam: 389 mg (74%). M_n(RI) = 6400, PDI = 1.39.

Kinetics of DbmOH and D,L-Lactide (Sn(oct)$_2$ Catalyst). The kinetics reaction was performed according to the procedure for **2** with Sn(oct)$_2$. The reaction was run in the bulk state at 130 °C at a loading of catalyst: initiator: monomer = 1/50: 1: 250. Aliquots were removed via pipet under N_2 at different time points and were analyzed without purification. GPC analysis with RI detection versus polystyrene standards was used to determine molecular weights (M_n) and polydispersity indices (PDIs). A correction factor of 0.58 was applied to M_n against polystyrene standards.[18] Monomer conversion and $-\ln[M]_t/[M]_0$ were calculated from the integration of GPC traces from RI detection corresponding to the polymer and monomer in the aliquots with the following equations, eqs 1 and 2. A correction factor of 0.89 was applied to the integration of the monomer peak, to account for the refractive index differences between lactide monomer and polymer.[12,19]

$$\text{conversion } \% = I_{\text{polymer}}/(I_{\text{polymer}} + 0.89I_{\text{monomer}}) \times 100\% \quad (1)$$

$$\begin{aligned} -\ln[\text{M}]_t/[\text{M}]_0 &= -\ln[0.89I_{\text{monomer}}/(I_{\text{polymer}} + 0.89I_{\text{monomer}})] \\ &= -\ln(1 - \text{conversion}/100) \end{aligned} \quad (2)$$

Kinetics of DbmOH and D,L-Lactide (DMAP Catalyst). The kinetics reaction was performed according to the procedure for that with Sn(oct)$_2$ but with DMAP as the catalyst.

Fe(dbmOH)$_3$ (3). A solution of dbmOH **1** (736 mg, 2.59 mmol) in THF (10 mL) was transferred by cannula to a flame-dried Schlenk flask containing NaH (62.4 mg, 2.59 mmol) in THF (10 mL). The suspension was stirred under nitrogen for 10 min, at which point no further evolution of gas was observed. Anhydrous $FeCl_3$ (140 mg, 0.86 mmol) was dissolved in THF (10 mL) in a Schlenk flask. The pale green iron solution was transferred via cannula to the reaction mixture containing **1** and NaH and the flask was washed with additional THF (~10 mL). The slightly cloudy dark red mixture was stirred for ~20 min, then passed through a medium frit and concentrated *in vacuo*. The residue was dissolved in CH_2Cl_2 (25 mL), the cloudy mixture was passed through Celite on a fine frit to clarify, and the red solution was concentrated *in vacuo*. The resulting solid was recrystallized from CH_2Cl_2/hexanes, was washed with hexanes, and then was redissolved in CH_2Cl_2, filtered through a fine frit, and dried *in vacuo* to give Fe(III)(1-[4-(2-hydroxy-ethoxy)-phenyl]-3-phenyl-propane-1,3-dione)$_3$ **3** as a dark maroon

crystalline solid: 0.508 g (65%). UV-vis ($CHCl_3$): λ_{max}(sh) = 480 nm, ε = 3 780 $M^{-1}cm^{-1}$. Anal. Calcd for $FeC_{51}H_{45}O_{12}$: C, 67.63; H, 5.01; Found: C, 67.79; H, 5.21. MS (ESI) m/z 906.4 $[M + 1]^+$.

Fe(dbmPLA)$_3$ (4) (Sn(oct)$_2$ Catalyst). A 10 mL flame-dried Kontes flask was charged with initiator **1** (24.5 mg, 27.6 μmol) and D,L-lactide (606 mg, 4.14 mmol). The flask was evacuated, backfilled with N_2, sealed, and lowered into an oil bath at 130 °C. Once a homogeneous melt was formed, Sn(oct)$_2$ in hexanes (50 μL of a 33.1 mM solution, 1.67 μmol) was added to the reaction mixture. The dark red melt was stirred for 10 min, cooled to room temperature, and precipitated from CH_2Cl_2/MeOH (3×) and CH_2Cl_2/hexanes (1×) to yield Fe(dbmPLA)$_3$ as a red-orange solid: 0.412 g, (65%). M_n(UV) = 14 100, PDI = 1.11.

Synthesis of Fe(dbmPLA)$_3$ (4) (DMAP Catalyst). The polymerization was performed according to the procedure for Fe(dbmPLA)$_3$ with Sn(oct)$_2$ except that DMAP (20.2 mg, 0.165 mmol) was used as the catalyst. The reaction mixture was stirred for 32 min, cooled to room temperature, and precipitated from CH_2Cl_2/MeOH (3×) and CH_2Cl_2/hexanes (1×) to yield Fe(dbmPLA)$_3$ as a red-orange solid: 0.738 g (62%). M_n(UV) = 17 600, PDI = 1.13.

Synthesis of Fe(dbmPLA)$_3$ (4) (No Catalyst). Fe(dbmPLA)$_3$ was prepared by the procedure described above for Fe(dbmPLA)$_3$ with Sn(oct)$_2$ except that no catalyst was added to the melt. After polymerization (10 min), the viscous mixture was precipitated from CH_2Cl_2/MeOH (3×) to yield a red-orange solid: 0.363 g (66%). M_n(UV) = 23 200, PDI = 1.06. UV−vis ($CHCl_3$): λ_{max}(sh) = 480 nm, ε = 3880 $M^{-1}cm^{-1}$.

Kinetics Studies of Fe(dbmOH)$_3$ and D,L-Lactide (No Catalyst). The kinetics reactions were performed at different temperatures according to the procedure for **2** with no added catalyst. Aliquots were removed via pipet under N_2 at intervals over a span of 40 min and were immediately dissolved in THF without purification for molecular weight characterization by GPC with UV−vis detection at 480 nm vs polystyrene standards. Percent monomer conversion was determined by ^{1}H NMR using relative integrations of the monomer methine −CH peak (centered at 5.02 ppm) vs the peak arising from the −CH− backbone protons of the polymer (centered at 5.16 ppm). The monomer conversion and $-\ln[M]_t/[M]_0$ were also calculated from the integration of GPC traces via RI detection and are in good agreement with the NMR method.

Fe(dbmPLA)$_3$ Homoblock Copolymers. Addition of D,L-Lactide to Fe(dbmPLA)$_3$. A 10 mL Kontes flask was charged with Fe(dbmPLA)$_3$ (M_n(UV) = 20 300; 15.4 mg, 0.735 μmol) and D,L-lactide (123.5 mg, 0.857 mmol). The flask was evacuated, backfilled with N_2, sealed and lowered into an oil bath at 130 °C. The red melt was stirred for 2.5 h, removed from the oil bath, and cooled to room temperature. The crude product was dissolved in CH_2Cl_2 (~3 mL) for precipitation from cold MeOH (~35 mL). The suspension was centrifuged, the mother liquor was decanted and the gummy solid was dried *in vacuo* to give a red solid: 32.7 mg, (24%, uncorrected for monomer consumption). M_n(UV) = 48 200, PDI = 1.07.

Demetalation. A 0.02 M HCl/THF solution (5 mL) (0.17 mL of concentrated aqueous HCl in 100 mL of THF) was added to a THF solution (5 mL) of Fe(dbmPLA)$_3$ (M_n(UV) = 28 800, PDI = 1.11, 503 mg, 17.5 μmol). After stirring for ~2 min, the reaction mixture was transferred to a separatory funnel containing CH_2Cl_2 (~200 mL). The organic layer was washed with brine (2 × 50 mL), dried over Na_2SO_4 and concentrated to ~5 mL *in vacuo*. Drop-wise addition of the resulting solution into cold hexanes (~35 mL) precipitated the polymer product. The mixture was centrifuged, the mother liquor was decanted, and the gummy solid was dried *in vacuo* to give a colorless solid: 0.376 g (72%). M_n(RI) = 10 500, PDI = 1.04. ^{1}H NMR data were the same as previously reported for dbmPLA.[20]

Coordination of DbmPLA to Iron(III). DbmPLA (M_n = 9100, PDI = 1.16, prepared by demetalation) (21.2 mg, 2.8 μmol) was dissolved in THF (2 mL). Et_3N (1 μL) was added, and the mixture was stirred for ~5 min. $FeCl_3 \cdot 6H_2O$ (220 μL, 4.2 mM solution in THF) was added and the resulting red-orange solution was stirred for ~10 min then added dropwise to cold MeOH (~35 mL). The heterogeneous mixture was centrifuged, the mother liquor was decanted, and the gummy solid was dried *in vacuo* to give the red-orange solid: 19.4 mg (92%). UV-vis ($CHCl_3$): λ_{max}(sh) = 480 nm, ε = 3840 $M^{-1}cm^{-1}$. M_n(UV) = 22 200, PDI = 1.07.

Kinetics of Benzyl Alcohol and D,L-Lactide (Fe(dbm)$_3$). A 10 mL Kontes flask was charged with D,L-lactide (1.08 g, 7.51 mmol) and Fe(dbm)$_3$ (23.3 mg, 32.1 μmol), evacuated, and backfilled with N_2. Benzyl alcohol (10 μL, 92.5 μmol) was injected under N_2 and the flask was lowered into an oil bath at 130 °C to produce a homogeneous melt. Aliquots were removed via pipet under N_2 at predetermined time points and were immediately dissolved in THF and characterized by GPC without purification. GPC analysis with RI detection versus polystyrene standards was used to determine molecular weights (M_n) and polydispersity indices (PDIs). Percent monomer conversion was determined from the integration of GPC traces from RI detection corresponding to the polymer and monomer of the aliquots. A correction factor of 0.89 was applied to the integration of the monomer peak, to account for the refractive index differences between lactide monomer and polymer. Kinetics studies with other iron β-diketonate catalysts were performed in the same way.

Results and Discussion

Macroligand Synthesis via Dibenzoylmethane Ligand Initiators. Stannous 2-ethylhexanoate (Sn(Oct)$_2$) is the most widely used catalyst for the controlled ROP of lactide.[21] Direct polymerizations of D,L-lactide from the primary alcohol-functionalized dbm derivative, 1-[4-(2-hydroxyethoxy)-phenyl]-3-phenyl-propane-1,3-dione (dbmOH, **1**), as the initiator, with Sn(oct)$_2$ as the catalyst were performed in bulk monomer at 130 °C as shown in eq 3. Low molecular weight dbmPLA macroligands **2** (M_n < 10 kDa) can be consistently produced with low PDIs (< 1.2).

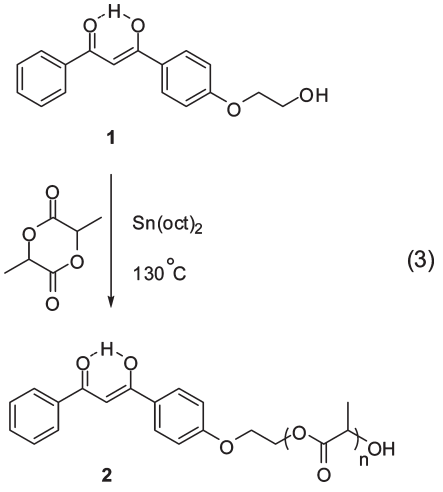

(3)

Two hydroxyl groups in the dbmOH molecule, the enol and the primary alcohol at the pendant chain end, can conceivably initiate the ROP of lactide. A short dbmPLA chain (~10 monomer units) prepared by the direct polymerization method was analyzed by ^{1}H NMR spectroscopy in $CDCl_3$ for end group structure identification (Figure 1). The formation of the ester functionality indicative of ROP initiation predominantly at the primary alcohol site instead of the enol was confirmed by the downfield shift of the signals associated with the adjacent methylene protons from 4.18 and 4.02 ppm to 4.51 (*f*) and 4.24 ppm (*g*) respectively. The resonance for the initiator primary alcohol at 1.97 ppm (*l*) was not observed. The signals from the enol group (16.95 ppm) and γ-H between the two carbonyls (6.80 ppm) were unaltered.

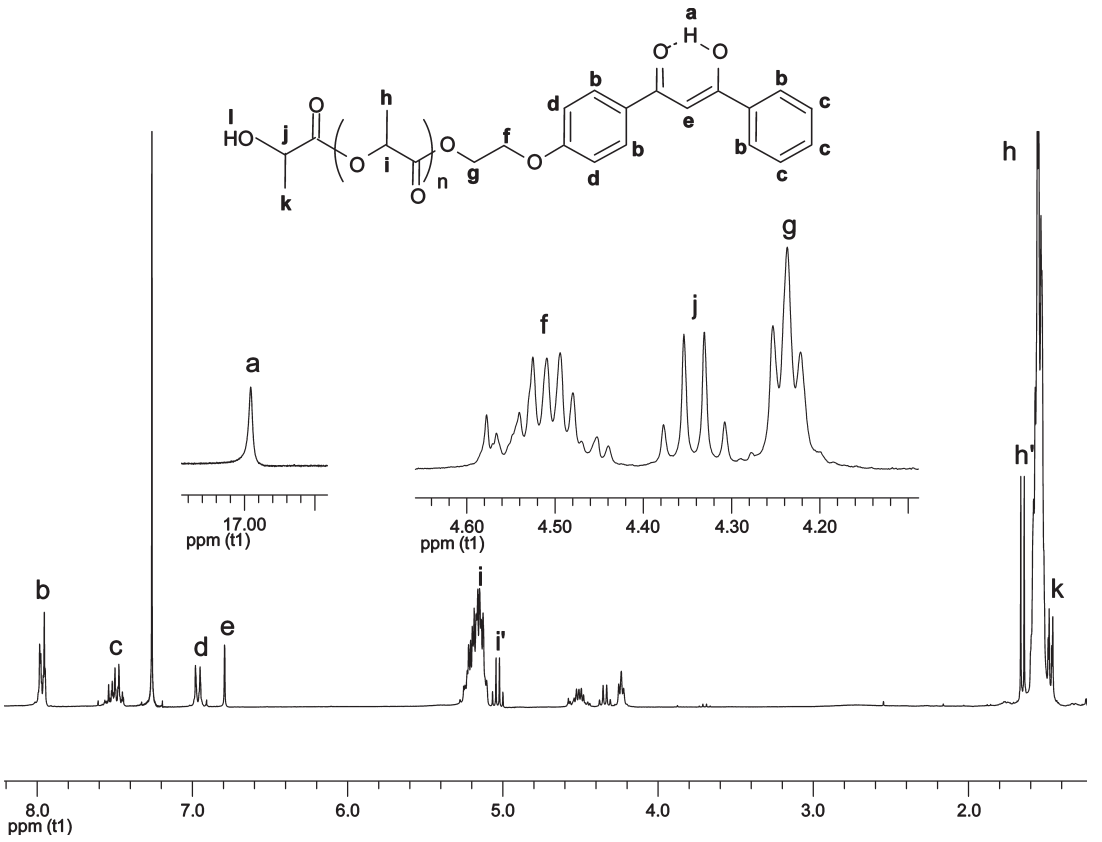

Figure 1. 300 MHz ^{1}H NMR spectrum in $CDCl_3$ for dbmPLA prepared with the $Sn(oct)_2$ catalyst. (h' and i' are methane and methine peaks from the lactide monomer.)

Kinetics studies were performed with the dbmOH initiator, D,L-lactide, and $Sn(oct)_2$ by analyzing reaction aliquots over time to provide quantitative information on reaction rate and molecular weight control. A linear correlation between M_n and monomer percent conversion was observed up to ~60% conversion, as shown in Figure 2a. PDIs were well below 1.20 throughout the polymerization. However, the observed molecular weights deviated from the calculated values based on monomer to initiator loading. High molecular weight shoulders in GPC traces were also observed at high monomer conversion, implying the presence of undesired side reactions, perhaps transesterication and thermal depolymerization. In Figure 2b, the $-\ln[M]_t/[M]_0$ vs time plot indicated that the reaction rate is rather low compared to those with common alcohol initiators,[22] and the plot is not linear, suggesting that the polymerization is not first order with respect to monomer loading. No induction period was observed. Similar phenomena were also observed in the polymerization of ε-caprolactone with the dbmOH initiator and $Sn(oct)_2$ catalyst.[15] Though low PDI polymers may be obtained upon reaction of cyclic esters with dbmOH using $Sn(oct)_2$ as the catalyst to generate PLA or PCL, the polymerizations are not entirely controlled.[23]

Previously, we have reported that coordination of tin to dbm may be responsible for altered catalyst activity and polymerization behavior for ε-caprolactone.[24] Since the diketone moiety is a good ligand for tin,[25] it may compete with the active propagating chain end for the tin center and significantly lower the effective concentration of the catalyst and otherwise alter its activity, leading to the decreased chain propagation rate and high molecular weight shoulder observed in GPC traces. It is also reported that at later time points in the polymerization of D,L-lactide with $Sn(oct)_2$, very slow Sn

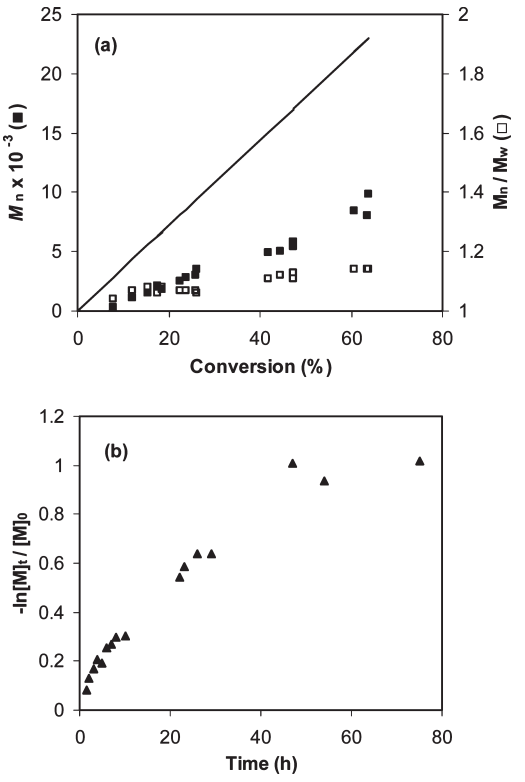

Figure 2. (a) Kinetics plot of M_n and PDI vs monomer percent conversion for D,L-lactide polymerization with the dbmOH initiator and the $Sn(oct)_2$ catalyst (line indicates calculated values based on initiator/monomer loading). (b) Kinetics plot of $-\ln[M]_t/[M]_0$ vs time. Polymerization performed at 130 °C in bulk monomer; catalyst:initiator:monomer = 1/50:1:250.

transfer between polymer chain ends in comparison to propagation could lead to bimodal peaks on GPC traces.[26]

The pendant $-OCH_2CH_2OH$ group on the dbm moiety could also serve as a bidentate ligand for the tin catalyst, forming a five-membered metallochelate ring and deactivate the catalyst. To rule out this possibility, the ketone precursor to dbmOH, *p*-$CH_3(CO)PhOCH_2CH_2OH$, was tested as the initiator with the $Sn(oct)_2$ catalyst under the same conditions. A polymer sample of $M_n = 10\,100$ and PDI = 1.14 was produced at 63% conversion in 40 min. The reaction time was significantly shortened in comparison to that with dbmOH as the initiator, suggesting that the pendant chain end is not responsible for the deactivation of the catalyst.

An alternative organocatalyst, 4-(dimethylamino)pyridine (DMAP), was also tested for the polymerization of lactide with dbmOH as the initiator. Much higher initiator-to-catalyst loading (1:2) is required than when using $Sn(oct)_2$.[11] The kinetics plot of M_n and PDI vs monomer conversion shown in Figure 3a indicates that the molecular weight control is rather poor. The molecular weights do not match the calculated values and molecular weight distribution is broad. However, the linear kinetics plot of $-\ln[M]_t/[M]_0$ vs time (Figure 3b) revealed that the reaction is still first order and faster than that with $Sn(oct)_2$ as the catalyst. GPC traces showed that high molecular weight shoulders were still observed. Since the acidity of protonated DMAP ($pK_a = 9.7$)[27] is very close to that of the enol in dbm ($pK_a = \sim 9$), it is likely that DMAP may also react with the enol, resulting in diminished control.

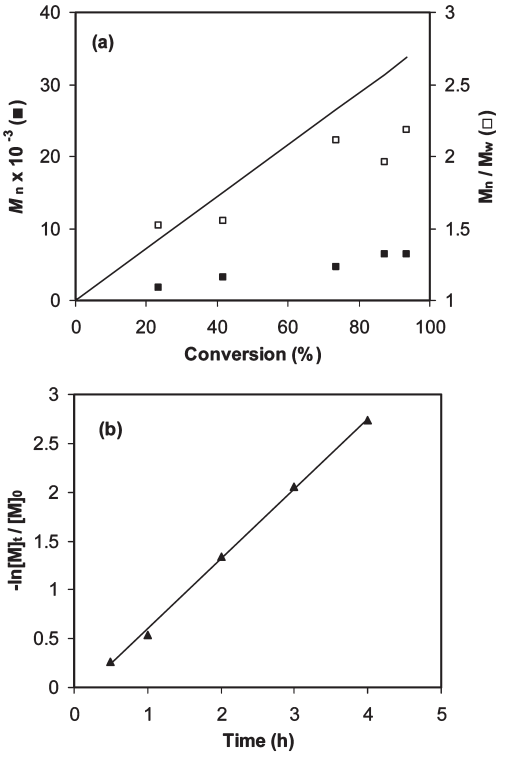

Figure 3. (a) M_n and PDI vs percent conversion plot for D,L-lactide polymerization with dbmOH initiator and DMAP catalyst (line indicates predicted results based on initiator/monomer loading). (b) Kinetics plot of $-\ln[M]_t/[M]_0$ vs time with the best fit line. Polymerization performed at 130 °C in bulk monomer; catalyst:initiator:monomer = 2:1:250.

Star Polymer Synthesis via Metalloinitiation. *Kinetic Studies*. One way to address the catalyst deactivation issue is to protect the enol coordination site in the dbm moiety.[28] An $Fe(dbmOH)_3$ complex **3** was synthesized from dbmOH and anhydrous $FeCl_3$ (eq 4). Iron tris(dbm) and related iron β-diketonate complexes are well-studied and their preparation is generally straightforward. Reaction of $Fe(dbmOH)_3$ metalloinitiator with D,L-lactide in the presence of $SnOct)_2$ or DMAP as the catalyst yielded iron-centered three-arm PLA stars, $Fe(dbmPLA)_3$, **4**. $Fe(dbmOH)_3$ dissolves in the lactide monomer melt to form a homogeneous polymerization mixture. Representative data are provided in Table 1. Reaction rates increased dramatically compared to those with dbmOH as the initiator. These findings also support the hypothesis that unprotected dbm can deactivate the catalyst by coordination.

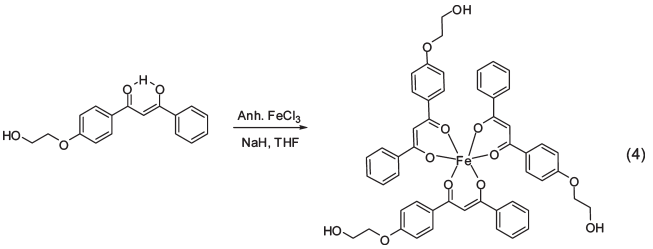

Surprisingly, polymerizations involving $Fe(dbmOH)_3$ and lactide with or without $Sn(oct)_2$ or DMAP gave polymer products at similar reaction rates. The iron complex is an effective catalyst by itself, eliminating the need for the additional reagents (eq 5). This could have implications for biomedical applications, since polymers obtained with trace catalysts can be more difficult to purify and are potentially hazardous to biological systems.[29] Therefore, $Fe(dbmOH)_3$ serves not only as an initiator and a dbm protecting group but also as a catalyst and potential bioactive agent, combining multiple functions in a single reagent.

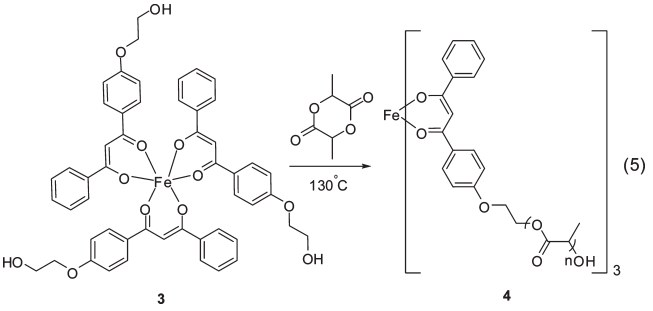

The polymerization of D,L-lactide from $Fe(dbmOH)_3$ initiator was monitored over time to explore the nature of the reaction. A linear correlation between M_n and conversion was observed up to about 70% conversion (Figure 4a).

Table 1. GPC Molecular Weight Data for $Fe(dbmPLA)_3$

	catalyst[a]	loading[b]	target M_n	M_n[c]	reaction time (min)	PDI[c]	yield (%)[d]
1	$Sn(oct)_2$	1:150	22 500	14 100	10	1.10	65
2	$Sn(oct)_2$	1:2000	288 000	62 800	45	1.24	20
3	DMAP	1:150	22 500	11 800	17	1.17	49
4	DMAP	1:300	44 100	17 600	32	1.13	62

[a] Reactions run in bulk at 130 °C. 1°ROH:$Sn(oct)_2$ = 1:1/150; 1°ROH:DMAP = 1:6. [b] Metalloinitiator-to-lactide monomer loading. [c] M_n and PDI were determined by GPC/UV−vis detection at 480 nm in THF with 0.58 correction factor applied to all M_n data. [d] Not corrected for monomer consumption.

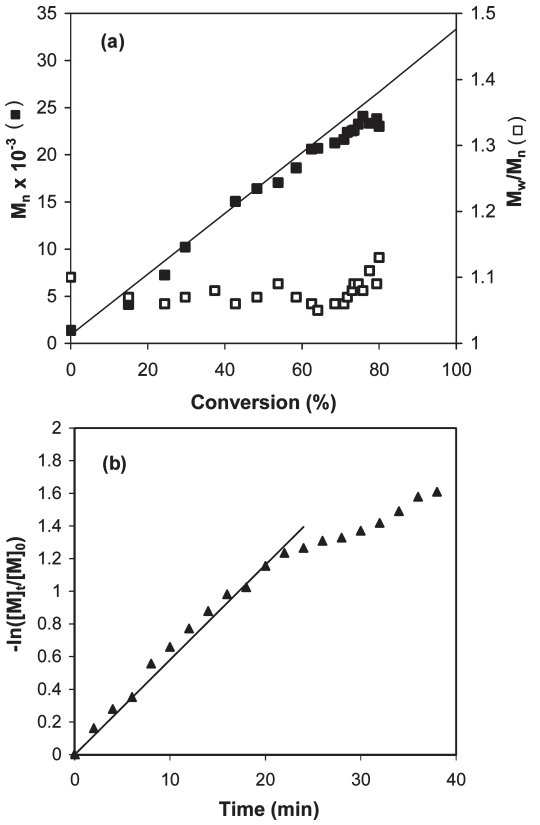

Figure 4. (a) Plot of M_n and PDI vs percent conversion for the polymerization of D,L-lactide with Fe(dbmOH)$_3$ initiator (line indicates calculated results based on initiator/monomer loading). (b) Kinetics plot of $-\ln[M]_t/[M]_0$ vs time; k_{app} = 0.053 min^{-1} (initiator-to-monomer ratio: 1:225).

The observed molecular weights were close to the calculated values, indicating that control is maintained for this system until a late stage of the polymerization. PDIs were well below 1.20, another indication of a controlled polymerization.[23] After this period when the reaction became viscous, molecular weight and PDI began to deteriorate. The corresponding $-\ln[M]_t/[M]_0$ vs time kinetics plot is shown in Figure 4b. The best fit line through the early time points of the reaction indicates that the reaction is first order in monomer loading (i.e., up to ~24 min time point), with an apparent rate constant k_{app} of 0.053 min^{-1} derived from the slope.

Polymerization temperature effects were also explored. Figure 5 compares the kinetics results from the polymerizations of D,L-lactide with the Fe(dbmOH)$_3$ initiator carried out at temperatures ranging from 130 to 180 °C at a fixed initiator-to-monomer ratio of 1:225. With elevated temperature, reaction rate increased rapidly. The highest molecular weight achieved increased with the temperature as well. However, at higher temperature, molecular weight control started to diminish, as reflected in the broadening molecular weight distributions, and molecular weights decreases from a certain peak value with time. This may be due to increased thermal depolymerization and transesterification at high temperatures.[32]

With kinetics data as a guide, preparative scale reactions were also performed to generate Fe(dbmPLA)$_3$ star polymers with different targeted molecular weights (Table 2). Kinetics studies show that reactions are well controlled at early stages of the polymerization, up to ~60−70% conversion. When higher conversion is targeted, high PDIs are observed. Previous studies have shown that viscosity increases at this point in the reaction,

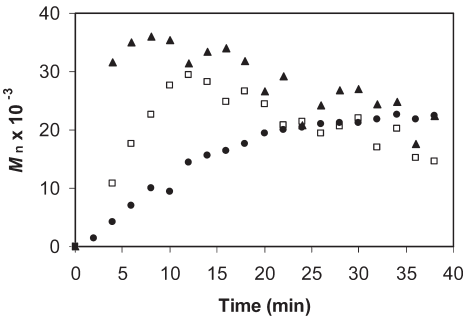

Figure 5. Plots of M_n and PDI vs time for the polymerization of D,L-lactide with Fe(dbmOH)$_3$ initiator at different temperatures (initiator-to-monomer ratio, 1:225; circle, 130 °C; square, 150 °C; triangle, 180 °C).

Table 2. GPC Molecular Weight Data for Fe(dbmPLA)$_3$ Prepared with No Additional Catalyst[a]

	target M_n[b]	loading	M_n[c]	PDI[c]	reaction time (min)	yield (%)[d]
1	10 800	1:75	7500	1.19	20	67
2	32 400	1:225	17 100	1.09	27	62
3	64 800	1:450	26 100	1.14	35	45
4	129 600	1:900	34 500	1.12	45	36
5	288 000	1:2000	64 700	1.22	60	22
6[e]	96 500	1:675	52 700	1.10	120	67

[a] Reactions run in bulk at 130 °C. [b] Metalloinitiator-to-lactide monomer loadings. [c] M_n and PDI were determined by GPC/UV−vis detection at 480 nm. 0.58 correction factor applied to all M_n data. [d] Not corrected for monomer consumption. [e] L-Lactide monomer.

causing the stir bar to stop stirring, which served as a rough indicator of when to stop the reactions. When higher molecular weights are targeted, reactions do not proceed to completion and lower yields are obtained. The iron complex can also be used as an initiator for the polymerization of L-lactide (Table 2, Entry 6).

Structural Analysis. The molecular weights and PDIs of the iron-centered polymers were determined by GPC with UV−vis detection at 480 nm (λ_{max} of the central Fe(dbm)$_3$) against polystyrene standards.[18] Refractive index (RI) detection was performed as well for comparison. A representative GPC overlay showing both RI and UV traces is provided in Figure 6a. The monomodal UV−vis trace (λ = 480 nm) shows that the metal-centered polymeric complex was obtained (M_n = 23 200, PDI = 1.06, ~70% monomer conversion). The RI trace, in contrast, is bimodal, with an approximately 3:1 M_n ratio between the two peaks, which corresponds to the macroligand-to-metal ratio of the Fe(dbmPLA)$_3$ polymeric complex. Because of the more compact nature of star polymers, their molecular weights are often underestimated if directly compared to linear polystyrene standards.[30] Correspondingly, the molecular weight of the large peak in the bimodal RI trace is often not strictly three times to that of the small peak, but slightly smaller. A 3D GPC plot obtained from UV−vis diode-array detection (DAD) provided in Figure 6b indicated that only the high M_n peak contains Fe(dbm)$_3$ chromophores ($\lambda_{max}(n \rightarrow d^*)$ = 480 nm), while dbm chromophores ($\lambda_{max}(\pi \rightarrow \pi^*)$ = 360 nm) are present in both. Partial ligand dissociation from Fe(dbmOH)$_3$ or Fe(dbmPLA)$_3$ during polymerization, purification or GPC analysis may explain these observations. Further characterization on the Fe(dbmPLA)$_3$ samples with GPC and UV−vis spectroscopy were performed to address the ligand dissociation issue. The extent of ligand dissociation in the polymeric complexes can be evaluated by the ratio r(GPC) of the integration of the large peak in the

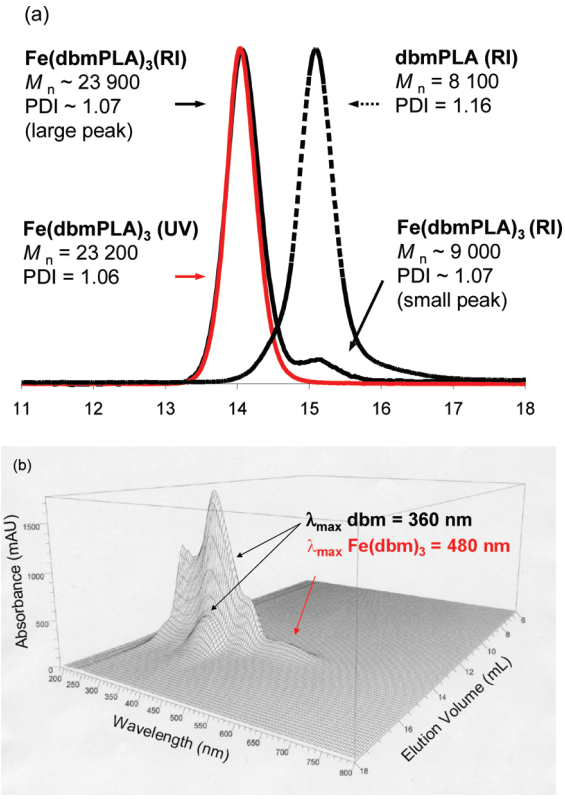

Figure 6. (a) GPC overlay of Fe(dbmPLA)$_3$ and the corresponding dbmPLA macroligand obtained after demetalation by acid treatment. Reprinted from ref 10. Copyright 2005 American Chemical Society. (b) 3D GPC plot of Fe(dbmPLA)$_3$ from UV−vis diode-array detector.

bimodal RI trace to that of the overall bimodal trace as defined in eq 6. However, accurate r(GPC) is difficult to obtain since the two RI peaks partially overlap. Extinction coefficients (ε) from UV−vis spectroscopy measured at wavelength corresponding to the n → d* transition of Fe(dbm)$_3$ were also employed. The ratio r(UV) of the extinction coefficient of the polymer sample to that of the Fe(dbmOH)$_3$ initiator (ε_0) is used as defined in eq 7 for comparison.

$$r(\mathrm{GPC}) = I_{\mathrm{large}}/(I_{\mathrm{large}} + I_{\mathrm{small}}) \quad (6)$$

$$r(\mathrm{UV}) = \varepsilon/\varepsilon_0 \quad (7)$$

A series of Fe(dbmPLA)$_3$ samples with different molecular weights were prepared and characterized with GPC and UV−vis spectroscopy. Data are provided in Table 3. GPC results indicate that the ratio of Fe(dbmPLA)$_3$ components r(GPC) slightly decrease with increasing M_n. The same trend is also observed for ε, but to a larger extent. No obvious correlation is found between r(GPC) and r(UV). This implies that the dissociation of the iron complex may not be the only reason for the decrease in extinction coefficient.

Solvent effects were also explored. Extinction coefficients of Fe(dbmPLA)$_3$ samples were measured in THF, methylene chloride and chloroform as shown in Table 4. Extinction coefficients decrease for this solvent series and also with increasing polymer molecular weight. Slightly smaller r(UV) values in THF may reflect an ability to form solvento complexes, with THF competing with the macroligand to bind to the central iron; however, solvation and stabilization of the polymer in the respective solvents is surely also playing a role. The mixtures after polymerization are purified by

Table 3. Comparison of GPC and UV-vis Data for Fe(dbmPLA)$_3$ with Respect to Complex-to-Macroligand Ratio

	M_n[a]	r(GPC)[b]	ε[c]	r(UV)[d]
1	11 500	0.91	4300	0.93
2	15 400	0.90	3500	0.76
3	22 200	0.92	3400	0.74
4	28 800	0.88	3100	0.67
5	38 700	0.86	3000	0.65

[a] Determined by GPC/UV−vis detection at 480 nm in THF. [b] r(GPC) = $I_{\mathrm{large}}/(I_{\mathrm{large}} + I_{\mathrm{small}})$. Calculated from GPC/RI detection. [c] Extinction coefficient determined by UV−vis spectroscopy at 480 nm in THF. Units: L mol^{-1} cm^{-1}. [d] r(UV) = $\varepsilon/\varepsilon_0$. ε_0 = 4 600 L mol^{-1} cm^{-1} at 480 nm in THF.

Table 4. Extinction Coefficients of Fe(dbmPLA)$_3$ Samples Compared to Fe(dbmOH)$_3$ Initiator in Different Solvents

	M_n[b]	PDI[b]	r(GPC)[c]	THF[d]	r(UV)[e]	CH_2Cl_2[f]	r(UV)	$CHCl_3$[g]	r(UV)
1[a]				4600		4300		3900	
2	23 800	1.17	0.84	3000	0.65	3000	0.70	2800	0.72
3	38 700	1.12	0.86	3000	0.65	3000	0.70	2700	0.69

[a] Fe(dbmOH)$_3$. [b] Determined by GPC/UV−vis detection at 480 nm in THF. [c] r(GPC) = $I_{\mathrm{large}}/(I_{\mathrm{large}} + I_{\mathrm{small}})$. Determined by GPC/RI detection in THF. [d] Measured at 480 nm in THF. [e] r(UV) = $\varepsilon/\varepsilon_0$. [f] Measured at 494 nm in CH_2Cl_2. [g] Measured at 492 nm in $CHCl_3$.

Table 5. GPC Data for Fe(dbmPLA)$_3$ Samples Before and After Precipitation[a]

	precipitation[b]	M_n[c]	PDI[c]	r(GPC)[d]
1	before	11 500	1.07	0.91
	after	11 800	1.07	0.92
2	before	15 400	1.06	0.90
	after	15 500	1.06	0.91
3	before	28 500	1.11	0.85
	after	28 700	1.11	0.87

[a] Samples were dissolved in CH_2Cl_2 and precipitated in cold methanol. [b] Before or after precipitation. [c] Determined by GPC/UV−vis detection at 480 nm in THF. [d] r(GPC) = $I_{\mathrm{large}}/(I_{\mathrm{large}} + I_{\mathrm{small}})$. Determined by GPC/RI detection in THF.

dissolving in CH_2Cl_2 and precipitating into cold methanol to remove the excess monomer. To rule out the possibility that the Fe(dbmPLA)$_3$ complexes may decompose during purification, GPC characterization of the polymer samples before and after precipitation were performed and data are shown in Table 5. No apparent molecular weight and r(GPC) changes were noticed, suggesting that the Fe(dbmPLA)$_3$ complexes are not altered by the precipitation process.

It has been known that large elastomer molecules can undergo shear degradation when separated using traditional GPC columns.[31] The polymer chains can be trapped in the pores of the column media and undergo fragmentation by shear force. This may also happen to star-shaped polymeric complexes with metal junctions, that polymer arms may be cleaved from the metal center by shear forces. By changing the temperature of the GPC columns, and hence the viscosity of the mobile phase as well as the column pressure, the chromatography of the samples may be altered by the possible shear degradation. The same Fe(dbmPLA)$_3$ sample was analyzed by GPC under different column temperatures ranging from 10 to 30 °C. Data are provided in Table 6. The M_n data are reported against the standard curve calibrated at 20 °C. The observed molecular weight increased along with the increasing column temperature, while no obvious change to the bimodal RI trace in terms of shape and r(GPC) was observed. So the effect of shear degradation under the current characterization conditions may be not detectable. These results suggested that the observed partial dissociation of Fe(dbmPLA)$_3$ may occur before column separation, probably due to the labile nature of the complex and the bulkiness of

Table 6. GPC Data for Fe(dbmPLA)$_3$ Samples at Different Column Temperatures.[a]

no.	temperature (°C)	M_n[b]	PDI[b]	r(GPC)[c]
1	10	14 700	1.07	0.92
2	20	15 300	1.07	0.92
3	30	16 100	1.07	0.91

[a] THF used as mobile phase. [b] Determined by GPC/UV−vis detection at 480 nm. [c] r(GPC) = $I_{large}/(I_{large} + I_{small})$. Determined by GPC/RI detection.

the macroligands. However, some details are still not fully understood, such as factors that lead to a decrease in extinction coefficient, and conditions that affect the chromatography with RI detection (r(GPC)). More studies are still required to address this issue and to obtain the fully chelated polymeric complexes.

To test whether polymers grown from the Fe(dbmOH)$_3$ initiator can serve as macroinitiators for further polymerization, that is, a criterion for living reactions,[23] a homo block copolymer was prepared via resubmission of more lactide monomer to a purified Fe(dbmPLA)$_3$. Specifically, a Fe(dbmPLA)$_3$ sample (M_n = 11 400, PDI = 1.12) was isolated and purified, and then resubmitted to reaction with 1000 equivalents of D,L-lactide at 130 °C. Large amounts of monomer were required to lower the viscosity of the reaction melt. Additional monomer units were added to the end of the polymeric metal complex starting material to produce a well-defined complex (M_n = 32 900, PDI = 1.13) after 75 min. The GPC trace overlay of the Fe(dbmPLA)$_3$ homopolymer sample before and after monomer addition is provided in Figure 7. The UV trace (Figure 7a) was shifted completely to lower elution volume, suggesting that the polymers with Fe(dbm)$_3$ centers were involved in the subsequent polymerization. Any unbound dbmPLA macroligand could, of course, influence the polymerization kinetics by competing with other ligands or monomer for metal binding. However, the bimodal RI trace of the homopolymer starting material was also shifted as expected for a higher molecular weight product, and collapsed into a monomodal peak after demetalation (M_n = 13 600, PDI = 1.11), suggesting that the majority of the PLA macroinitiators participated in the subsequent polymerization (Figure 7b). The metal-free macroligand peak, possibly due to fragmentation of the metal star during or after polymerization or chain extension of dbmPLA in the macroinitiator mixture, is largely coincident with the dbmPLA generated by intentionally demetalation of the star polymer. Low molecular weight tailing in the RI traces upon monomer addition, however, may suggest that initiation from metal-free macroligand in the mixture is less controlled than chain extension from iron-centered stars. These findings indicate that the hydroxy chain ends and iron catalyst embedded in polymeric Fe(dbmPLA)$_3$ remain active.

Although the polymerization of D,L-lactide from Fe(dbmOH)$_3$ does not adhere to all of the criteria for a living reaction throughout the polymerization process,[23] it is still possible to prepare Fe(dbmPLA)$_3$ samples with targeted molecular weights and low PDIs based on insights from kinetics information. However, the partial ligand dissociation issue, whether it occurs during the reaction and/or on the GPC column still needs to be addressed in order to obtain homogeneous polymer reaction products.

Microstructure and Transesterification Analysis. End group analysis was conducted using ^{1}H NMR spectroscopy. A low molecular weight Fe(dbmPLA)$_3$ sample (~30 monomer units) was prepared by the reaction of Fe(dbmOH)$_3$ and D,L-lactide. To eliminate the paramagnetic effect of Fe(III) in NMR analysis, the crude product was demetalated by treating with 0.02 M HCl THF solution and extracted with water before

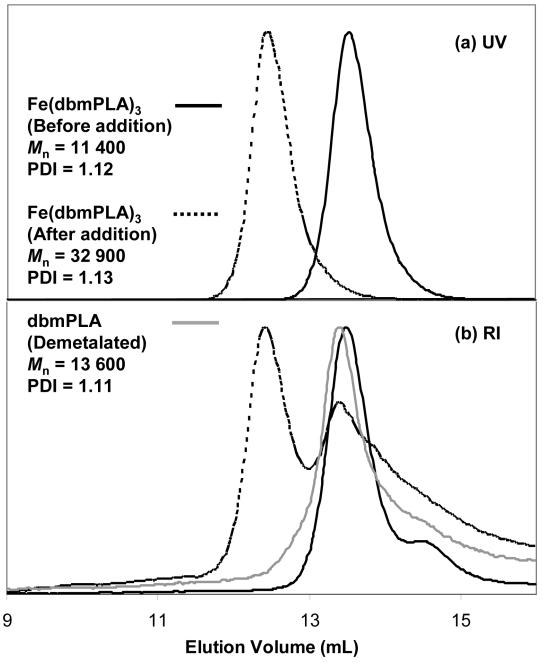

Figure 7. GPC overlay showing (a) UV−vis (detection at 480 nm) and (b) RI traces in THF of Fe(dbmPLA)$_3$ before and after addition of lactide to generate a homoblock copolymer.

characterization. Resonances are assigned as shown in Figure 8. Evidence of free dbmOH and lactide is still present (e.g., f', g' and i' peaks), probably from unreacted starting materials or a hydrolysis product of dbmPLA after demetalation. Signal a of the enol proton at 16.95 ppm is still apparent and signal e of γ-H at 6.80 ppm is unshifted, while the signals from the methylene protons of $-OCH_2CH_2OR$ shifted downfield from f' (4.18 ppm) and g' (4.02 ppm) (R = H in the dbmOH initiator) to f (4.52 ppm) and g (4.25 ppm)(R = $-C(O)CH(CH_3)O-$ in the dbmPLA polymer). The resonance of the initiator primary alcohol (~1.97 ppm) is not observed. These results indicate the presence of lactide polymer at the primary alcohol site rather than the enol metal coordinate site, which is a similar structure to dbmPLA prepared with Sn(oct)$_2$ mentioned before (Figure 1).

NMR spectroscopy is also employed to identify the stereostructure of the polymer backbone from stereosensitive resonances, so that information such as stereoselectivity of the initiator and the extent of transesterification and racemization can be obtained. Previously, ^{13}C NMR spectroscopy was frequently employed to detect the carbonyl and methine carbons of PLA, which are sensitive to the stereo environment. However, ^{1}H NMR spectra with a significantly better signal-to-noise ratio as compared to ^{13}C NMR spectra can provide better quantification of stereosequence probabilities. But due to the coupling between the methyl protons and the methine protons at each of the stereocenters, the splitting of the methine resonance becomes extremely complicated and difficult to interpret, as seen in Figure 1 and Figure 8 signal i. Homonuclear decoupling of the methyl protons can significantly reduce the splitting and simplify the spectral analysis.

The polymerization of D,L-lactide from the Fe(dbmOH)$_3$ initiator was monitored over time and homonuclear decoupled ^{1}H NMR spectra were recorded as shown in Figure 9 with stereoconfigurations assigned as previously reported.[32] NMR spectra were acquired at 500 MHz for best resolution. Normalized intensities of all the peaks were calculated and shown in Table 7, together with molecular weight data from

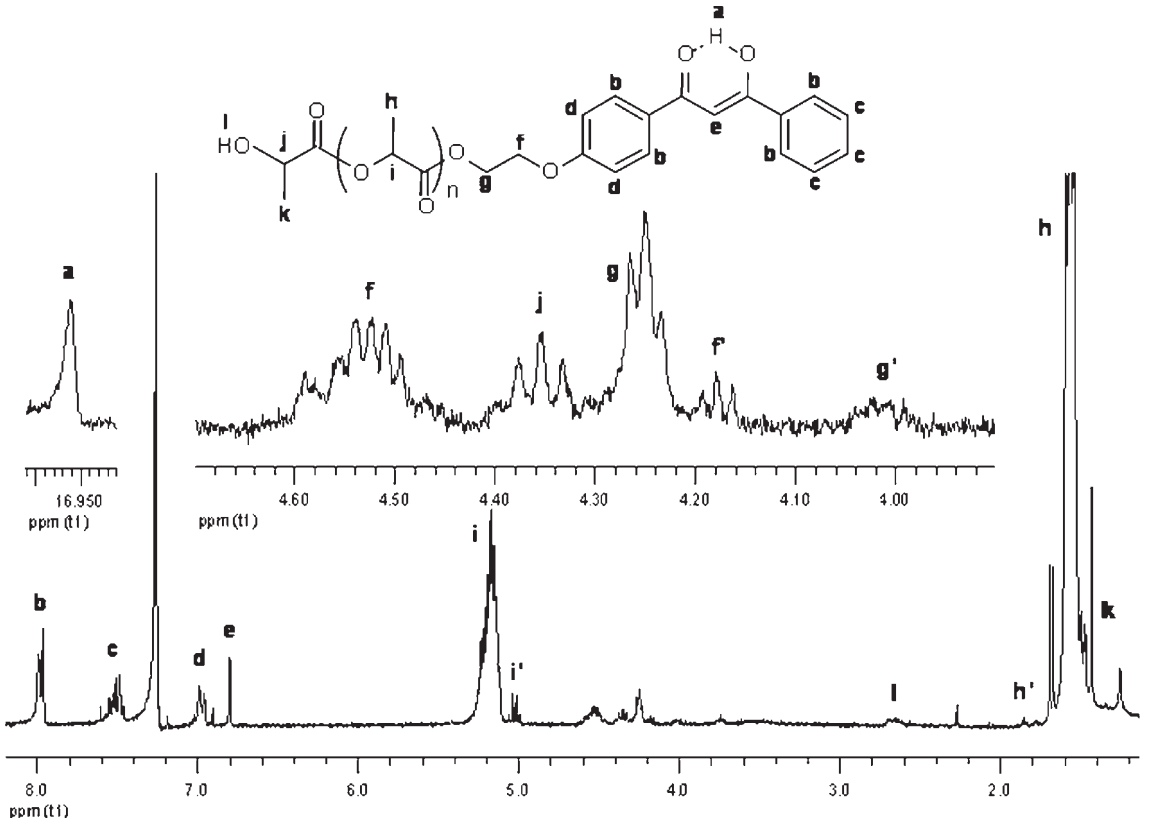

Figure 8. ^{1}H NMR spectrum in $CDCl_3$ of low molecular weight dbmPLA generated by demetalation of Fe(dbmPLA)$_3$ with 0.02 M HCl in THF (the integration ratio between b and k is 4:3).

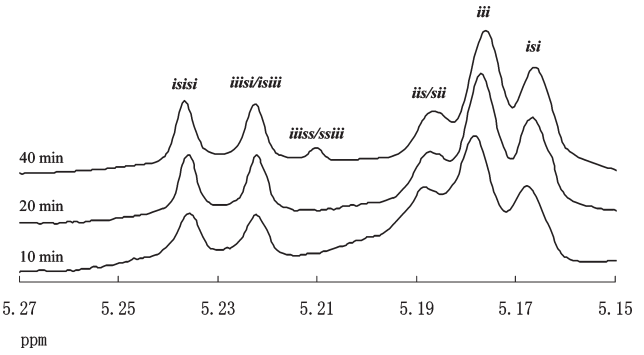

Figure 9. Methine resonance overlay in the homonuclear decoupled 500 MHz ^{1}H NMR spectra of Fe(dbmPLA)$_3$ samples over time. Note evidence of forbidden *iiiss*/*ssiii* sequences at ~5.21 ppm at the 40 min (78% monomer conversion) time point.

Table 7. GPC Data and Normalized Peak Intensities of Homonuclear Decoupling NMR Experiment for Fe(dbmPLA)$_3$ versus Reaction Time[a]

				hexads			tetrads		
time (min)	M_n[b]	PDI	conversion (%)	*isisi*	*isiii*/ *iiisi*	*iiiss*/ *ssiii*	*iis*/ *sii*	*iii*	*isi*
10	12 400	1.06	22	9	8	0	27	38	18
20	24 200	1.09	42	10	10	0	16	40	24
40	31 600	1.19	63	10	11	1	13	39	26

[a] Reactions run in bulk at 130 °C. Fe(dbmOH)$_3$:D,L-lactide = 1:225. [b] M_n, PDI, and conversion were determined by GPC/UV−vis detection at 480 nm. A 0.58 correction factor was applied to all M_n data.

GPC of the corresponding aliquots. During the polymerization process, the two well-resolved peaks representing hexad stereosequences of *isisi* and *iiisi*/*isiii* at 5.235 and 5.225 ppm respectively have nearly equal intensity. P_i, referred to as the probability of forming a new *i*-dyad, is frequently employed as a coefficient to measure the initiator stereoselectivity. Here the P_i of the Fe(dbmOH)$_3$ initiator calculated from the normalized intensities of hexads *isisi* and *iiisi*/*isiii* or tetrad *iii* according to the literature is 0.52.[33] On the basis of the prediction of the pairwise Bernoullian statistics for D,L-lactide, these observations suggested that the polymerization is close to random, or that possibly the Fe(dbmOH)$_3$ initiator exhibits only very slight isotactic stereoselectivity.[33]

The extent of transesterification can also be evaluated on the basis of the intensity of the stereosequence in the NMR spectra. A tiny peak at 5.21 ppm in the 40 min aliquot is assigned as the *iiiss*/*ssiii* unpaired stereosequences,[32] which are theoretically forbidden by the pairwise addition mechanism. Thus, they are considered to be the product of transesterification or racemization.[34] The transesterification coefficient (T), expressed by the ratio I_{iss}/I_{max}, allows a quantitative evaluation on the degree of transesterification, where I_{max} is the maximal intensity of an *iss* tetrad in a completely transesterified poly(D,L-lactide), which is 12.5% as calculated from the single-addition mechanism of Bernoullian statistics. A transesterification coefficient of 0.08 is obtained at 40 min, showing that Fe(dbmOH)$_3$ exhibits mild activity for transesterification in the polymerization of D,L-lactide. This effect only appears at the late stage of the polymerization (conversion >60%), when the viscosity of the reaction mixture increased, molecular weight control diminished and the PDI broadened. The same experiment was also performed with optically pure L-lactide as the monomer. However, only a singlet peak was observed; no evidence of racemization was found even at 78% conversion. Since the catalyst only exhibits slight stereoselectivity

Table 8. GPC Data for Representative Demetalated DbmPLA Samples

no.	M_n(Fe(dbmPLA)$_3$)[a]	PDI[a]	M_n(dbmPLA)[b]	PDI[b]	yield, %
1	37 500	1.10	13 700	1.27	92
2	32 000	1.06	11 100	1.17	63
3	28 800	1.11	10 500	1.04	72

[a] GPC/UV−vis detection at λ = 480 nm with 0.58 correction factor. [b] GPC/RI detection with 0.58 correction factor.

and should react similarly with either D-lactide or L-lactide, this result supports the assertion that transesterification, not racemization, is operative at the late stages of D,L-lactide polymerization, when sequences forbidden in the pairwise mechanism become apparent.

Demetalation. The Fe(dbmOH)$_3$-initiated polymerizations of D,L-lactide are effective for the production of Fe(III)-centered homopolymers and block copolymers, but some applications of interest require metal-free systems, as in luminescence studies of dbmPLA[17] or use as macroligands for coordination to metals other than iron (e.g., europium star polymers).[15] Therefore, complete removal of iron from the center of the star polymers without degrading the polymer backbone is crucial to the development of these materials for other applications and a number of demetalation conditions were tested. Ethylenediamine tetraacetic acid (EDTA) (log K_{stab}[Fe(EDTA)$^-$] = 24), salicylic acid (log K_{stab}[Fe(SA)$_3^{3-}$] = 42), oxalic acid (log K_{stab}[Fe(ox)$_3^{3-}$] = 20) and sodium cyanide (NaCN) (log K_{stab}[Fe(CN)$_6^{3-}$] = 42), which are known to form stable Fe(III) complexes as well as β-diketones (e.g., log K_{stab}[Fe(acac)$_3$] = 27),[35] were tested as reagents for this purpose, to cleave the polymeric iron complex. Each was stirred in THF solution with a red Fe(dbmPLA)$_3$ star polymer. No obvious color change was observed and red polymer products were obtained after precipitation in methanol. Under these conditions, none of these reagents were successful in removing the Fe from the polymeric material. Hydrochloric acid (HCl) is a common reagent for hydrolyzing metal complexes, particularly for the demetalation of metal-containing polymers[36] or for removal of iron catalysts from polymer products.[37] However, in the case of Fe(dbm)$_3$-centered polyesters, acid may also promote the hydrolysis of the polymer chains, cleaving the backbones and producing oligomers. A study was undertaken to screen for the optimal reaction conditions for complete demetalation of Fe(dbmPLA)$_3$ with HCl while minimizing the hydrolysis of the polymer. Solutions of aqueous hydrochloric acid in tetrahydrofuran were prepared in the following concentrations: 1, 0.1, 0.01, and 0.001 M. When added to a THF solution of Fe(dbmPLA)$_3$, the first three solutions became orange-red when the polymer was completely dissolved, and then turned colorless within seconds. The weakest hydrochloric acid solution, with a molarity of 0.001 M was stirred for 5 days with Fe(dbmPLA)$_3$, but no visual change in color was observed. The demetalation process does not appear to be molecular weight-dependent; samples of all molecular weight turned colorless at about the same rate when shaken with acid. Once clear and colorless, each solution was immediately transferred to a separatory funnel containing CH_2Cl_2. The organic layer was then washed with water twice and concentrated. The final dbmPLA products were obtained by precipitating the concentrated product from CH_2Cl_2/hexanes to give a white powder. The polymer product shows essentially no absorption at 480 nm, suggesting that the Fe(dbm)$_3$ chromophore has been effectively removed (Figure 6). However, UV−vis analysis verifies whether demetalation is complete; if for a given reaction, a signal is still evident at 480 nm, the demetalation process must be repeated. GPC with UV−vis detection at 360 nm reveals that the dbm chromophore remains associated with the polymeric samples and that dbm-functionalized macroligands were obtained. This is also confirmed by ^{1}H NMR spectroscopy (Figure 8). Additional evidence that the dbm binding sites are present in the demetalated polymers is provided by rechelation to Fe(III) to give red-orange products with UV−vis spectra consistent with those of the original Fe(dbmPLA)$_3$ stars. GPC data of representative dbmPLA samples from demetalation are shown in Table 8. Molecular weights of dbmPLA achievable by this demetalation/acidic deprotection method surpass those possible by polymerization from dbmOH with Sn(oct)$_2$. Yields are nearly quantitative and result in macroligands with relatively low PDIs. The M_n values corresponding to demetalated dbmPLA are often slightly more than one-third of the parent Fe(dbmPLA)$_3$ complex, likely due to the compact nature of the star polymer in GPC analysis as previously mentioned.[30]

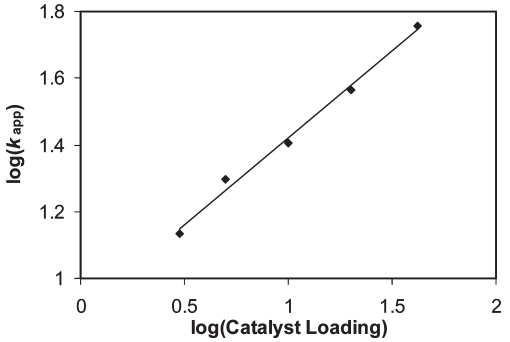

Figure 10. Plot of log(k_{app}) vs log(catalyst loading), with the best fit line to eq 8.

Control Study. It is reported that other metal β-diketonates, such as the acetylacetonates of aluminum,[38] zinc,[34] iron,[39] zirconium,[40] and tin[41] have been successfully employed as catalysts in lactide polymerizations. To better understand the mechanism of Fe(dbmOH)$_3$ as the initiator for lactide polymerization, a comparison study using benzyl alcohol and dbmOH as initiators and exogenous Fe(dbm)$_3$ as the catalyst was performed. For the benzyl alcohol initiator, polymerizations were run at 130 °C at a fixed initiator-to-monomer loading of 1:75 while the Fe(dbm)$_3$ catalyst loading was varied. The presence of the benzyl alcohol end group structure in the final product was confirmed by ^{1}H NMR analysis of the purified polymers. Aliquots were taken via pipet at predetermined time points and were analyzed by GPC with RI and UV−vis detection at 480 nm. The polymerizations proceeded similarly to those using Fe(dbmOH)$_3$ as the initiator with respect to rate. GPC results indicated that the Fe(dbm)$_3$ chromophore is not coincident with polymer RI peaks as is seen when Fe(dbm)$_3$ chromophores are incorporated into the polymer; however, the red catalyst remained entrapped in the polymer product after precipitation, which previously has been associated with a coordination−insertion mechanism.[42] All reactions exhibited a linear correlation in M_n vs percent monomer conversion plots and $-\ln[M]_t/[M]_0$ versus time to ~70% conversion. The apparent rate constant (k_{app}) for each run was obtained from the slope of the best-fit line to the plot of $-\ln([M]_t/[M]_0)$ versus time for all points with PDI ≤ 1.2. For these polymerizations, a plot of k_{app} vs catalyst loading in molar ratio is nonlinear, as shown in Figure 10. A best fit curve corresponds to the following equation:

$$\log(k_{app}) = 0.90 + 0.52 \log(\text{catalyst loading}) \qquad (8)$$

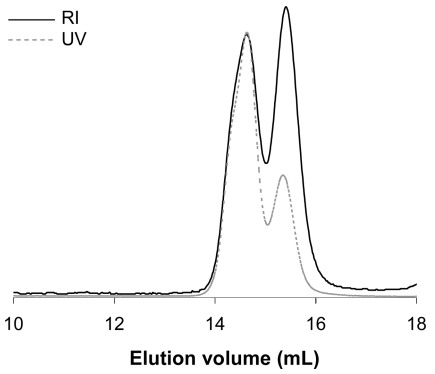

Figure 11. Overlay of RI and UV−vis (λ = 480 nm) traces for dbmOH-initiated PLA using Fe(dbm)$_3$ as catalyst. (Note from the UV trace the presence of the Fe(dbm)$_3$ chromophores in both polymer peaks).

Kinetics plots suggest that the order in Fe(dbm)$_3$ catalyst is approximately one-half (0.52). Such fractional order dependency on the catalyst is not uncommon for cyclic ester polymerizations and is widely believed to arise from the aggregation of active polymer chains, for which the propagation rate is either slower (order <1) or faster (order >1) than the non-aggregated species.[43] It is reported that aggregation during polymerization processes leads to poor molecular weight control and hinders propagation. This is commonly seen for iron compounds such as alkoxides[43] and carboxylates[36] used as catalysts for lactide polymerizations.

Another possible reason for the fractional order may be an alcohol/catalyst interaction in the initiation process. It is possible that the benzyl alcohol might react with Fe(dbm)$_3$ by ligand exchange; a proton transfer from the alcohol to dbm ligand could generate an iron alkoxide species and free, or partially dissociated dbm. Similar ligand exchange and proton transfer phenomena were observed when Zr(acac)$_4$ was used as the catalyst for glycolide−lactide copolymerization.[44] An "in situ" generated iron alkoxide could serve as the initiating species for reaction with lactide monomer via a coordination−insertion mechanism to produce the actively propagating chain end.[40]

DbmOH was also tested in conjunction with Fe(dbm)$_3$ to determine if this catalyst system would allow for faster rates and/or better molecular weight control than the Sn-based catalyst to prepare high molecular weight dbmPLA products. Reaction times for these dbmOH-initiated polymerizations with Fe(dbm)$_3$ were comparable or slightly longer than those employing Sn(oct)$_2$ as the catalyst. As with the metalloinitiated Fe(dbmPLA)$_3$ samples, a bimodal RI peak was seen in the GPC trace for each of these samples. Interestingly, GPC analysis employing the UV−vis detector at λ = 480 nm revealed a bimodal trace corresponding to the Fe(dbm)$_3$ chromophore coincident with the RI polymer trace, as shown in Figure 11. Given that Fe(III) diketone complexes undergo ligand exchange,[45] this can explain the presence of Fe in the polymer. The dbmPLA macroligands that are formed may exchange with the nonpolymeric dbm ligands on the Fe catalyst during the course of the reaction to produce a product mixture that can be represented by the molecular formula Fe(dbm)$_x$(dbmPLA)$_{3-x}$, where $x = 0-3$.

As is the case with preparations of Fe(dbmPLA)$_3$ from Fe(dbmOH)$_3$, the molecular weight ratio between the two peaks is between 1:2 and 1:3 for dbmPLA samples prepared using Fe(dbm)$_3$ as the catalyst. This suggests that given the formula above, x = 1 and 2 for the low molecular weight peak, and the higher molecular weight peak is a combination of samples in which $x = 0$. Also, the discrepancy between RI and UV intensities for the right peak suggests a mixture of metal-bound and metal-free macroligand. After precipitation of the crude product into cold methanol to remove unreacted monomer, the red-orange color remained. As for the Fe(dbmPLA)$_3$ samples prepared by metalloinitiation from Fe(dbmOH)$_3$, acid treatment was used to dissociate the macroligands from the Fe center to obtain dbmPLA. This process affords macroligands that give rise to a monomodal GPC RI trace with no evidence by UV−vis of Fe(dbm)$_3$ chromophores coincident with the polymer peak. In the polymerizations using Fe(dbmOH)$_3$ as the initiator, since dbmOH can be regarded as an ambidentate ligand, it is conceivable that the labile iron β-diketonate complex can first undergo a linkage isomerization to an iron alkoxide by an intramolecular or bridging intermolecular process.[46] An iron alkoxide thus generated may then serve as the initiator for the lactide polymerization. This partial degradation of Fe(dbm)$_3$ centers that may be necessary to generate an active initiator and catalyst may also help to explain the biomodal RI traces and extinction coefficient decreases in Fe(dbmPLA)$_3$ samples compared to the Fe(dbmOH)$_3$ starting material.

An additional control experiment where only Fe(dbm)$_3$ and lactide were added at 130 °C was also performed. Even without added alcohol initiators, polymerization does occur. Polymeric species with molecular weights up to 40 kDa were obtained after 10 min. GPC coupled with UV-vis spectroscopy was used to monitor the polymerization products. However, the polymeric species did not show any absorption in the UV-vis range, suggesting that neither dbm or Fe(dbm)$_3$ were incorporated into the resulting polymer on the chain ends. This does not rule out initiation from these species; however, if the end group is susceptible to cleavage from the chain end during the polymerization or work up, or that Fe(dbm)$_3$ may be serving as a catalyst for impurity-initiated lactide polymerization.

Several iron compounds such as iron alkoxide,[42] FeCl$_3$,[47] and Fe(acac)$_3$[39] have been employed as catalysts for the polymerization of lactide with or without additional alcohol initiators, and typically act as Lewis acids to activate the monomer carbonyl. However, high temperature and long reaction time are often needed, polymerizations are not controlled, and molecular weight distribution is generally broad. Because Fe(dbm)$_3$ has been found to serve as an efficient catalyst in lactide polymerization from benzyl alcohol as mentioned above, a series of substituted iron β-diketonate complexes including iron acetylacetonate (Fe(acac)$_3$), iron benzylacetylacetonate (Fe(bzac)$_3$) and iron trifluoroacetylacetonate (Fe(tfa)$_3$) (Figure 12) were also tested as the catalysts for the same reaction in order to screen for the best catalyst and also to explore the structure−activity relationship of the different iron β-diketone complexes as catalysts for ROP of lactide.

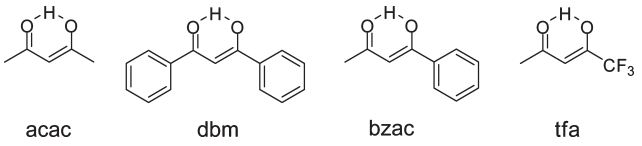

Figure 12. β-Diketonate ligands used to make iron catalysts for ROP of D,L-lactide.

Table 9. Apparent Rate Constants and Ligand pK_a of Different Iron β-Diketonates for D,L-Lactide ROP

catalyst	Fe(acac)$_3$	Fe(dbm)$_3$	Fe(bzac)$_3$	Fe(tfa)$_3$
k_{app} (min^{-1})	0.1325	0.0705	0.0530	0.0209
ligand pK_a[a]	9.7	9	9.8	6.7

[a] Reference 48.

All reactions were run at the same loading of catalyst: initiator: monomer = 1/3:1:75 at 130 °C in bulk and were monitored over time. Linear kinetics plots of M_n and PDI vs percent monomer conversion and $-\ln[M]_t/[M]_0$ vs time were obtained at the early stage of polymerization (up to ~70−80% conversion, PDI ≤ 1.2). The apparent rate constant for each catalyst was derived from the slope of a fit straight line to the $-\ln[M]_t/[M]_0$ vs time plot for all data points with PDI ≤ 1.2. Polymerizations for each catalyst were run twice and the average rate constants are provided in Table 9. The order of reaction rate is $Fe(acac)_3 > Fe(dbm)_3 > Fe(bzac)_3 > Fe(tfa)_3$, approximately decreasing with increasing enol acidity of the corresponding β-diketone ligands also shown in Table 9 except for $Fe(bzac)_3$. These results suggest that iron metalloinitiators with β-diketonate ligands besides dbm could also be effective in self-catalyzing polymerization reactions.

Conclusions

In summary, $Fe(dbmOH)_3$ was synthesized for use as the metalloinitiator for D,L-lactide polymerization. The iron complex plays multiple roles in the synthesis of $Fe(dbmPLA)_3$ and its component dbmPLA macroligands, serving as a protecting group, initiator, catalyst, activating group, functional elements (i.e., chromophores or reactive centers) and potentially bioactive agents in the resulting material. Polymeric $Fe(dbmPLA)_3$ complexes can be prepared efficiently with no additional catalyst. Kinetics studies indicated good molecular weight control up to high monomer conversion (~70%). NMR spectroscopy was employed to study the end group structure and stereosequence distribution, indicating that $Fe(dbmOH)_3$ exhibits only very slight stereoselectivity and transesterification activity at high monomer conversion. Demetalation with HCl produces dbmPLA macroligands suitable for chelation to other metals. Model studies with BnOH and dbmOH as the initiators were conducted with a series of iron β-diketonate complexes to further explore the mechanism of the polymerization, revealing evidence of ligand exchange under the reaction conditions. These studies advance fundamental understanding of coordination chemistry with polymeric ligands and show promise for responsive polymer applications in the fields of biomedicine and materials science.

Acknowledgment. We thank the NSF (CHE 0350121 and CHE 0718879) and DuPont for support for this research.

References and Notes

(1) Fraser, C. L.; Smith, A. P. *J. Polym. Sci., Part A: Polym. Chem.* **2000**, *38*, 4704–4716.
(2) Marin, V.; Holder, E.; Hoogenboom, R.; Schubert, U. S. *Chem. Soc. Rev.* **2007**, *36*, 618–635.
(3) Hoogenboom, R.; Schubert, U. S. *Chem. Soc. Rev.* **2006**, *35*, 622–629.
(4) Thomas, M. C. *Chem. Soc. Rev.* **2010**, *39*, 165–173.
(5) Kricheldorf, H. R.; Sumbel, M. V.; Kreiser-Saunders, I. *Macromolecules* **1991**, *24*, 1944–1949.
(6) Kricheldorf, H. R.; Berl, M.; Scharnagl, N. *Macromolecules* **1988**, *21*, 286–293.
(7) Platel, R. H.; Hodgson, L, M.; Williams, C. K. *Polym. Rev.* **2008**, *48*, 11–63.
(8) Fairbank, V. F.; Fahey, L. L. *Clinical Disorders of Iron Metabolism*; Grune-Stratton: New York, 1971.
(9) Tatarsky *PCT Int. Appl.* WO 2003004014, **2003**.
(10) Gorczynski, J. L.; Chen, J.; Fraser, C. L. *J. Am. Chem. Soc.* **2005**, *127*, 14956–14957.
(11) Dechy-Cabaret, O.; Martin-Vaca, B.; Bourissou, D. *Chem. Rev.* **2004**, *104*, 6147–6176.
(12) Kowalski, A.; Duda, A.; Penczek, S. *Macromolecules* **1998**, *31*, 2114–2122.
(13) Kricheldorf, H. R.; Hachmann-Thiessen, H.; Schwarz, G. *Biomacromolecules* **2004**, *5*, 492–496.
(14) Yuan, M.; Li, X.; Xiong, C.; Deng, X. *Eur. Polym. J.* **1999**, *35*, 2131–2138.
(15) Bender, J. L.; Shen, Q.-D.; Fraser, C. L. *Tetrahedron* **2004**, *60*, 7277–7285.
(16) Gorczynski, J. L. Ph.D. Thesis, University of Virginia, **2005**.
(17) Zhang, G.; Evans, R. E.; Campbell, K. A.; Fraser, C. L. *Macromolecules* **2009**, *42*, 8627–8633.
(18) Save, M.; Schappacher, M.; Soum, A. *Macromol. Chem. Phys.* **2002**, *203*, 889–899.
(19) Biela, T.; Duda, A.; Rode, K.; Pasch, H. *Polymer* **2003**, *44*, 1851–1860.
(20) Bender, J. L.; Corbin, P. S.; Fraser, C. L.; Metcalf, D. H.; Richardson, F. S.; Thomas, E. L.; Urbas, A. M. *J. Am. Chem. Soc.* **2002**, *124*, 8526–8527.
(21) Schwach, G.; Coudane, J.; Engel, R.; Vert, M. *Polym. Bull.* **1994**, *32*, 617–623.
(22) For example, polymerization of D,L-lactide with ethylene glycol as the initiator and $Sn(oct)_2$ as the catalyst at 130 °C at a loading of catalyst:initiator:monomer = 1/25:1:300, M_n = 21 800, PDI = 1.06, and reaction time 12 min.
(23) Quirk, R. P.; Lee, B. *Polym. Int.* **1992**, *27*, 359–367.
(24) Bender, J. L.; Shen, Q.-D.; Fraser, C. L. *Tetrahedron* **2004**, *60*, 7277–7285.
(25) Saxena, P. N.; Saxena, Sanjiv. *Appl. Organomet. Chem.* **1989**, *3*, 279–281.
(26) Penczek, S.; Duda, A.; Szymanski, R. *Macromol. Symp.* **1998**, *132*, 441–449.
(27) Höfle, G.; Steglich, W.; Vorbrüggen, H. *Angew. Chem., Int. Ed. Engl.* **1978**, *17*, 569–583.
(28) McAlvin, J. E.; Scott, S. B.; Fraser, C. L. *Macromolecules* **2000**, *33*, 6953–6964.
(29) Schwach, G.; Coudane, J.; Engel, R.; Vert, M. *J. Polym. Sci., Part A: Polym. Chem.* **1997**, *35*, 3431–3440.
(30) http://www.wyatt.com/literature/irontris.pdf (Accessed November 20, **2009**)
(31) http://www.wyatt.com/literature/butadi.pdf (Accessed November 20, **2009**).
(32) Thakur, K. A. M.; Kean, R. T.; Hall, E. S.; Kolstad, J. J.; Lindgren, T. A.; Doscotch, M. A.; Siepmann, J. I.; Munson, E. J. *Macromolecules* **1997**, *30*, 2422–2428.
(33) Coudane, J.; Ustariz-peyret, C.; Schwach, G.; Vert, M. *J. Polym. Sci., Part A: Polym. Chem.* **1997**, *35*, 1651–1656.
(34) Bero, M.; Kasperczyk, J.; Jedlinski, Z. J. *Makromol. Chem.* **1990**, *191*, 2287–2296.
(35) Dean, J. A. *Lange's Handbook of Chemistry*, 13th ed.; McGraw Hill Book Company: New York, 1985.
(36) Saunders, G. D.; Foxon, S. P.; Walton, P. H.; Joyce, M. J.; Port, S. N. *Chem. Commun.* **2000**, 273–274.
(37) Stolt, M.; Södergard, A. *Macromolecules* **1999**, *32*, 6412–6417.
(38) Bero, M.; Kasperczyk, J.; Adamus, G. *Makromol Chem* **1993**, *194*, 907–912.
(39) Wang, X.; Liao, K.; Quan, D.; Wu, Q. *Gaofenzi Xuebao* **2005**, *1*, 113–118.
(40) Dobrzynski, P. *J. Polym. Sci., Part A* **2004**, *42*, 1886–1900.
(41) Nijenhuis, A. J.; Grijpma, D. W.; Pennings, A. J. *Macromolecules* **1992**, *25*, 6419–6424.
(42) Wang, X.; Liao, K.; Quan, D.; Wu, Q. *Macromolecules* **2005**, *38*, 4611–4617.
(43) O'Keefe, B. J.; Breyfogle, L. E.; Hillmyer, M. A.; Tolman, W. B. *J. Am. Chem. Soc.* **2002**, *124*, 4384–4393.
(44) Dobrzynski, P.; Kasperczyk, J.; Janeczek, H.; Bero, M. *Macromolecules* **2001**, *34*, 5090–5098.
(45) Ivanchenko, V. A.; Nekipelov, V. M. *React. Kinet. Catal. Lett.* **1984**, *32*, 263–267.
(46) Sekine, T.; Inaba, K. *Bull. Chem. Soc. Jpn.* **1984**, *57*, 3083–3087.
(47) Arvanitoyannis, I.; Nakayama, A.; Psomidou, E.; Kawasaki, N.; Yamamoto, N. *Polymer* **1996**, *37*, 651–660.
(48) Calvin, M.; Wilson, K. W. *J. Am. Chem. Soc.* **1945**, *67*, 2003–2007.